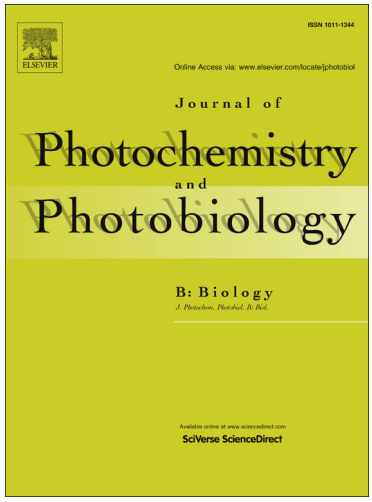

Electrochemical and spectroscopic investigations of carboxylic acid ligand and its triorganotin complexes for their binding with ds.DNA: In vitro biological studies

Nasima Arshad, Shahid Iqbal Farooqi, Moazzam H. Bhatti, Samreen Saleem, Bushra Mirza

PII: S1011-1344(13)00105-X
DOI: http://dx.doi.org/10.1016/j.jphotobiol.2013.05.005
Reference: JPB 9496

To appear in: *Journal of Photochemistry and Photobiology B: Biology*

Received Date: 20 February 2013
Revised Date: 8 May 2013
Accepted Date: 10 May 2013

Please cite this article as: N. Arshad, S.I. Farooqi, M.H. Bhatti, S. Saleem, B. Mirza, Electrochemical and spectroscopic investigations of carboxylic acid ligand and its triorganotin complexes for their binding with ds.DNA: In vitro biological studies, *Journal of Photochemistry and Photobiology B: Biology* (2013), doi: http://dx.doi.org/10.1016/j.jphotobiol.2013.05.005

Electrochemical and spectroscopic investigations of carboxylic acid ligand and its triorganotin complexes for their binding with ds.DNA: In vitro biological studies

Nasima Arshad[a,*], Shahid Iqbal Farooqi[a], Moazzam H. Bhatti[a], Samreen Saleem[b], Bushra Mirza[b]

[a] Department of Chemistry, Allama Iqbal Open University, Islamabad, Pakistan

[b]Department of Biochemistry, Quaid-i-Azam University, Islamabad, Pakistan

[a,*]Corresponding author. Tel.: +92 51 9057756; fax: +92 51 9250081.

E-mail address: nasimaa2006@yahoo.com (Nasima Arshad)

A B S T R A C T

A carboxylic acid ligand, (*Z*)-4-(4-acetylphenylamino)-4-oxobut-2-enoic acid (APA-1), and its triphenyl- (APA-2) and tributyl-tin(IV) (APA-3) compounds have been synthesized and investigated for their binding with ds.DNA using UV-visible spectroscopy, fluorescence spectroscopy, cyclic voltammetry, and viscosity measurements under physiological conditions of pH and temperature. The experimental results from all techniques *i.e.* binding constant (K_b), binding site size (n) and free energy change (ΔG) were in good agreement and inferred spontaneous compound–DNA complexes formation *via* intercalation. Among all the compounds APA-3 showed comparatively greater binding at pH 4.7 as evident from its greater K_b values {APA-3: K_b: 5.63×10^4 M^{-1} (UV); 7.94×10^4 M^{-1} (fluorescence); 9.91×10^4 M^{-1} (CV)}. Electrochemical processes of compounds before and after the addition of DNA were found diffusion controlled. Among all compounds, APA-3 exhibited best antitumor activity.

Key words: Triorganotin(IV) carboxylates, UV-visible / fluorescence spectroscopy, cyclic voltammerty, intercalation, binding constant / site size, bioactivities

1. Introduction

A vital role of DNA in life processes is to direct all the cell's activities including genetic information related to cellular function, DNA replication and gene expression. However, it can easily be damaged under some conditions [1]**.** DNA damage is the fundamental cause of mutations leading to cancer. Its control is one of the most important and big issue to be resolved. Numerous researches have been carried out to discover most effective anticancer agents and to utilize them as drug candidates. Recent trends to control or inhibit nucleic acid damage mainly emphasis on the interaction of DNA with other molecules; especially certain classes of drugs and metal complexes. Chemotherapeutic anti-cancerous treatment involves the inhibition of the rapid cell division by targeting DNA through covalent or non-covalent interactional modes [2]. Among both interactional modes, reversible types non-covalent binding is preferred over covalent adduct formation due to less chance of toxic side effects of the drug candidate [3]. Normally, three types of non-covalent binding modes are considered in DNA binding studies: (i) electrostatic interaction with the phosphate ions of DNA backbone, (ii) groove binding and (iii) intercalation of the compound into the stacked base pairs of DNA. Spectroscopic and electrochemical methods have proven to be more authentic and frequently employed methods to anticipate the mode of interaction of small molecules as well as metal complexes via non covalent binding [4−7].

Among metal complexes, organotins have gained much attention due to their high therapeutic and biomedical applications and have extensively been studied for their interaction with DNA in order to develop new and effective candidates as anticancer drug [8−11]. Organotin compounds containing a carboxylic group are considered to have potential biocidal and cytotoxic activities [12, 13]. However organotin carboxylates are certainly very promising for cancer

chemotherapy [14, 15]. They have extensively been studied and screened in vitro and vivo for antitumor activity [12, 16−18]. As a result divinyl, di-n-butyl, tri-n-butyl, and triphenyltin carboxylates are found to be more active than *cis*-platin in vitro against different human cell lines [19]. Generally, triorganotin(IV) carboxylates have shown much higher biological activities when compare to their mono- and di-organotin(IV) analogues due to high binding ability to proteins [20].

Hence due to tremendous importance of organotin carboxylates, present research has been focused to investigate binding interactions of (*Z*)-4-(4-acetylphenylamino)-4-oxobut-2-enoic acid (APA-1) and its triphenyl- and tributyl-tin(IV) compounds {(triphenylstannyl (*Z*)-4-(4-acetylphenylamino)-4-oxobut-2-enoate (APA-2), tri-n-butylstannyl (*Z*)-4-(4-acetylphenyl-amino)-4-oxobut-2-enoate (APA-3)} with ds.DNA using UV-visible spectrometry, fluorescence spectroscopy, cyclic voltammetry, and viscosity measurements. These compounds were also investigated for their antioxidant and antitumor potential by using different bioassays.

2. Experimental

2.1. Materials

All reagents were procured from Aldrich / Fluka and used without further purification. All the solvents were dried before use by the literature methods. The ligand (APA-1) and its two complexes APA-2 and APA-3 were prepared as given in scheme 1. ds.DNA was extracted in the laboratory from chicken blood by the Falcon method [21] and its concentration was determined spectrophotometrically at 260 nm using molar extinction coefficient, ε_{260} = 6600 $cm^{-1}M^{-1}$ [22]. Purity of DNA was checked by monitoring the ratio of the absorbance at 260 nm to that at 280 nm and solution gave a ratio of A_{260}/A_{280} > 1.8, indicating that DNA was sufficiently pure and

free from protein [23]. The stock solutions of APA-1, APA-2, and APA-3 were prepared by dissolving them in buffer solution of pH 4.7 (acetate buffer; CH_3COOH + CH_3COONa) and pH 7.4 (phosphate buffer; Na_2HPO4 + NaH_2PO_4). Autoclaved water was used to prepare all the solutions.

2.2. Instrumentation

The melting points were determined in capillary tubes using a MPD Mitamura Riken Kogyo (Japan) Electro thermal melting point apparatus and were uncorrected. FTIR spectra (KBr) were recorded on Nicolet iS 10 FTIR spectrophotometer in the range 4000 − 400 cm^{-1}. The ^{1}H and ^{13}C NMR spectra were recorded on a Bruker Avance 400 spectrometer operating at 400 MHz. The electronic absorption spectra were recorded on Shimadzu 1800 spectrophotometer (TCC-240A, Japan) equipped with temperature control device using 1.0 cm matched quartz cells. Fluorescent emission spectra were recorded on F-7000 FL spectrophotometer 2133-007. Cyclic voltammetric experiments were performed using AUTOLAB PGSTAT–302 with GPES version 4.9 (Eco Chemie, Utrecht, Netherlands).

Electrochemical measurements were carried out in a dried conventional three electrode cell using a glassy carbon (GCE; d = 3 mm) working electrode, a saturated calomel (SCE; 3.5 M KCl) reference electrode and a Pt sheet counter electrode. Prior to each experiment the GCE was polished with alumina powder and rinsed thoroughly with doubly distilled water for 30 seconds.

2.3. Preparation of compounds

2.3.1. Synthesis of Ligand acid (APA-1)

The ligand acid was obtained from the reaction of maleic anhydride with *p*-aminoacetophonene in ethyl acetate as shown in Scheme 1. A solution of maleic anhydride (1.0 g, 10 mmol) in 50 ml ethyl acetate was added to a solution of *p*-aminoacetophonene (1.35 g, 10

mmol) in 50 ml ethyl acetate in a 250 ml conical flask. The mixture was stirred for three hours at room temperature. After stirring the precipitates of ligand acid were filtered and recrystallized with ethanol.

Scheme 1

2.3.2. Synthesis of of APA-2 and APA-3

The organotin derivatives APA-2 and APA-3 were obtained from the reaction of Ph_3SnOH / $(Bu_3Sn)_2O$ with ligand acid in 1:1 and 1:2 molar ratio, respectively. All the newly synthesized compounds are air stable, crystalline solids and soluble in common organic solvents. The general chemical reaction is given as Scheme 2.

For the preparation of APA-2, equimolar amounts of ligand acid (2.33 g, 10 mmol) and triphenyltin hydroxide (3.17 g 10.mmol), while for the preparation of APA-3 molar amounts (2:1) of ligand acid (2.33 g, 10 mmol) and bis(tributyltin)oxide (3.17 g 10.mmol) respectively were suspended in 100 ml of dry ethanol / acetone (8:2) solvent mixture and refluxed for 8 hours,. After cooling to room temperature, reaction mixture was filtered and solvents were evaporated in rotary evaporator. The solid obtained was recrystallized from chloroform with few drops of *n*-hexane.

Scheme 2

2.3.3. Characterization data

Physical data APA-1: Yield 78 %, m.p.: 210-212 °C. FTIR data (KBr, cm^{-1}): ν (OH) 3300-2900, ν (NHCO) 1709, ν (CH_3CO) 1674, ν_{asym} (COO) 1631, ν_{sym} (COO) 1362, $\Delta\nu = 269$

^1H NMR data (DMSO, ppm $^3J(^1H, ^1H)$ in Hz): 12.9 (b, 1H, CONH), 10.6 (s, 1H, COOH), 7.92 (d, 2H, (8.0), aromatic protons), 7.73 (d, 2H, (8.0), aromatic protons), 6.47 (d, 1H, (12), ethylene proton), 6.31 (d, 1H, (12), ethylene proton), 2.52 (s, 3H, CH_3CO)

^{13}C NMR data (DMSO, ppm): 166.9 (C1), 130.3 (C2), 131.5 (C3), 196.5 (C4), 143 (C5), 129.5 (C6), 118.6 (C7), 132.0 (C8), 163.6 (C9), 26.4 (C10)

Physical data APA-2: Yield 67 %, m.p.: 180-182 °C. FTIR data (KBr, cm^{-1}): ν (CH_3CO) 1675, ν (NHCO) 1620, ν_{asym} (COO) 1590, ν_{sym} (COO) 1372, Δν = 218, ν (Sn-O) 452

^{1}H NMR data ($CDCl_3$, ppm $^{3}J(^{1}H, ^{1}H)$ in Hz): 11.5 (b, 1H, CONH), 7.88 (d, 2H, (8.4), aromatic protons), 7.55 (d, 2H, (8.4), aromatic protons), 7.74-7.70 & 7.50-7.45 (m, 15H, SnPh), 6.36 (d, 1H, (13.4), ethylene proton), 6.28 (d, 1H, (13.4), ethylene proton), 2.57 (s, 3H, CH_3CO)

^{13}C NMR data ($CDCl_3$, ppm, $^{n}J[^{119}Sn, ^{13}C]$ in Hz): 171.9 (C1), 129.2 (C2), 129.6 (C3), 197.0 (C4), 142.5 (C5), 127.5 (C6), 119.2 (C7), 132.9 (C8), 162.3 (C9), 26.4 (C10), 138.2 [661] (Cα), 136.8 [46.8] (Cβ), 130.7 [66.4] (Cγ), 132.9 (Cδ)

Physical data APA-3: Yield 62 %, m.p.: 78-80 °C. FTIR data (KBr, cm^{-1}): ν (CH_3CO) 1678, ν (NHCO) 1612, ν_{asym} (COO) 1592, ν_{sym} (COO) 1368, Δν = 224, ν (Sn-C) 582, ν (Sn-O) 450

^{1}H NMR data ($CDCl_3$, ppm $^{3}J(^{1}H, ^{1}H)$ in Hz): 12.3 (b, 1H, CONH), 7.90 (d, 2H, (8.4), aromatic protons), 7.71 (d, 2H, (8.2), aromatic protons), 6.28 (d, 1H, (13.6), ethylene proton), 6.23 (d, 1H, (13.2), ethylene proton), 2.55 (s, 3H, CH_3CO), 1.64-1.59 & 1.35-1.29 (m, 18H, $SnCH_2CH_2CH_2$), 0.88 (t, 9H, $SnCH_2CH_2CH_2CH_3$)

^{13}C NMR data ($CDCl_3$, ppm, $^{n}J[^{117/119}Sn, ^{13}C]$ in Hz): 171.5 (C1), 129.0 (C2), 129.6 (C3), 197.0 (C4), 143.0 (C5), 132.8 (C6), 119.2 (C7), 137.6 (C8), 162.6 (C9), 26.4 (C10), 17.1 [333/349] (Cα), 27.7 [21.2] (Cβ), 27.0 [65.4] (Cγ), 13.6 (Cδ)

2.4. Procedure for analysis

2.4.1. UV-visible and fluorescence spectroscopic titrations

Concentration of DNA determined spectrophotometrically (UV-spectroscopy) at 260 nm was found 1.8×10^{-4} M. Spectroscopic titrations were carried out at stomach pH (4.7) and blood (7.4) under body temperature (37 °C). The absorbance measurements by UV-visible spectrophotometer and the fluorescence emission spectra by fluorescence spectrophotometer were recorded by keeping the concentration of APA-1, APA-2 and APA-3 constant (2.8×10^{-5} M) in the sample cell, while varrying the concentration of ds.DNA from 10 μM to 60 μM in the sample cell. In order to achive the equilibrium between the compound and DNA, solutions were allowed to stay for at least 5 minutes before each measurements were made. After placing the sample solutions within the cell cavity and before runnig the spectra, wait for a few seconds till required temperature was attained and shown on temperature controlled device.

2.4.2. Voltammetric assay

First a blank CV was run with the buffer solutions (4.7 and 7.4) at 37 °C, which showed no electroactivity in the potential range of our interest (−2 V to +2 V). Cyclic voltammograms of APA-1, APA-2 and APA-3 (2.8×10^{-5} M) were recorded from −2.0 V to +1.0V *vs.* SCE before and after the addition of different volumes (μl) of the stock DNA solution corresponding to the final concentration of DNA ranging from 10 μM – 60 μM within the cell. Scan rate of 100 mV/s was used throughout the experiments. All measurements were made at 37 °C after purging the solution in the cell with argon gas (99.999%) for at least 10 to 15 min for flushing out oxygen before every electrochemical assay.

2.4.3. Viscosity measurements

Initially viscosity of DNA solution (η_o) was determined at stomach (4.7) and blood (7.4) pH under physiological temperature (37 °C). Then specific viscosity contribution (η), due to DNA (10 μM) in the presence of increasing concentration of investigated compound was

determined. The values of the relative specific viscosities for the compounds i.e. $(\eta / \eta_o)^{1/3}$ were then plotted against the ratio; [compound] / [DNA].

2.4.4. DPPH free radical scavenging assay

DPPH free radical scavenging activity of test compounds were carried out by already reported methods [24, 25]. Compounds were examined at four concentrations 7.4, 22.2, 66.6 and 200 µg ml^{-1} as final concentrations from stock. Reaction mixture was prepared by adding 0.1 ml of each test compound solution in DMSO, 2 ml of 0.1 mM DPPH in ethanol solution and 0.9 ml of 50 mM Tris-HCl in capped vials. DMSO was used as negative and ascorbic acid was used as positive control, respectively. Reaction mixture was incubated in dark for 30 minutes at room temperature. After incubation, change in DPPH color was observed by spectrophotometric absorbance at 517 nm. Mixture of all solvents utilized in the assay was used as blank for the spectrophotometer. Percent scavenging of DPPH free radical for each concentration of each compound was calculated.

2.4.5. Potato disc antitumor assay

Potato disc antitumor assay with some modifications was performed to detect the tumor inhibition activity of compounds under investigation [5, 24, 25]. In this assay 48 hour old single colony culture of *Agrobacterium tumefaciens* (At-10) strain was used as tumor inducing agent on potato discs. Each test sample was evaluated for antitumor activity at four concentrations i.e., 7.4, 22.2, 66.6, and 200 µg ml^{-1} with DMSO as negative controls and vincristine as standard drug. Under complete aseptic conditions, potato discs (0.5 cm thickness) were made by using sterilized instruments from surface sterilized ($HgCl_2$ 0.1%) healthy potatoes tubers. Fifteen potato discs were transferred on each petriplate containing 1.5% agar–agar in distilled water. After treatment with test compounds and At-10 strain on each disc, these petriplates were then

incubated at 28°C for 21 days. Number of tumors was counted after staining with the Lugol's solution (10% KI and 5% I_2) with the help of dissecting microscope. Percentage tumor inhibition was calculated. Each experiment was carried out in triplicate and IC_{50} values for each compound were calculated.

3. Results and discussion

3.1. DNA binding study by UV-spectroscopy

UV-visible spectrophotometry is the most significant technique to study the binding mode of small molecules as well as metal complexes [26]. The comparison of UV-visible spectra of compounds in the absence and presence of DNA provides an efficient tool for monitoring and recognition of their interaction and yield information about compound−DNA binding mechanism and complex formation [26]. Three compounds APA-1, APA-2and APA-3 have been analyzed spectrophotometrically to get an insight into their interactions with ds-DNA at physiological conditions of pH and temperature.

At first, UV-spectrum of APA-1, APA-2, APA-3 all having same concentration (2.8×10^{-5} M) were recorded separately in the complete UV-visible range (200 – 800 nm), Fig. S1 (in supplementary information). All solutions were prepared in ethanol-water mixture (7:3). A single peak appears at λ_{max} of 307.2 nm, 304.4 nm and 314.8 nm respectively for APA-1, APA-2 and APA-3 compounds respectively. The molar extinction coefficient (ε) values were evaluated 11175 $cm^{-1}M^{-1}$, 16292 $cm^{-1}M^{-1}$and 10300 $cm^{-1}M^{-1}$ respectively for APA-1, APA-2 and APA-3 and predicted that π-π^* transitions are operative for all compounds in the λ_{max} range 240 – 390 nm, Figs. S2 and S3 (concentration profile; in supplementary information). Absorption spectrum of pure chicken blood ds-DNA recorded in double deionized distilled water showed a broad band

(200 – 350 nm) in the UV-region with a maximum placed at 260 nm. The observed maximum is the consequence of the chromophoric groups in purine and pyrimidine moieties. The absorbance ratio (A_{260}/A_{280}) was 1.83, which ensured the purity of DNA [23].

Addition of varying concentration of DNA (10 μM − 60 μM) on fixed (optimized) concentration (2.8×10^{-5} M) of APA-1, APA-2 and APA-3 caused progressive blue shift of magnitude 3.0 nm, 4.2 nm and 8 nm respectively at pH 4.7 and 1.2 nm, 3.0 nm and 4.9 nm respectively at pH 7.4 in the electronic absorption spectra along with the decrease in peak absorbance intensity (hypochromic effect) at both pH, Fig. 1. Such changes in the spectral responses are indicative of binding of investigated compounds with DNA [8]. Hypochromism in absoption spectra after the addition of DNA is suggestive of intercalation of these compounds into the DNA base pairs and this may probably be due to the interaction of the electronic states of the intercalating chromophore of the compounds and those of the stacked base pairs of ds-DNA via overlapping [27, 28]. On the other hand, the coupling π-orbital is partially filled by electrons, thus decreasing transition probabilities and concomitantly resulting in hypochromism [27, 28].

Furthermore, upon titration with DNA the spectral changes at both the pH are characterized by one isosbestic point, Fig. 1, so presence of species other than the free and the intercalated complexes could be ruled out [18]. Isosbestic point indicates that there is equilibrium between bound DNA and the free form of the compounds and further suggested only one mode of binding i.e., intercalation of compounds with DNA [29].

Fig. 1

3.2. DNA binding study by fluorescence-spectroscopy

Fluorescence-spectroscopy is one of the important technique to probe compound-DNA binding [5, 30]. The intrinsic fluorescence emission spectra of APA-1, APA-2 and APA-3 were recorded separately and all the compounds were found luminescent, Fig. S4 (in supplementary information). Hence binding studies were carried out by direct addition of different concentrations of DNA.

The intrinsic fluorescence emission spectra of all the compounds were recorded separately before and after the addition of varying concentrations of DNA and the effect on the fluorescence emission spectra of compounds; APA-1, APA-2 and APA-3 is given in Fig. 2. Upon addition of DNA (10 μM – 60 μM), the growth of emission intensities of APA-1, APA-2 and APA-3 is recorded larger than those in the absence of DNA as 2.07, 2.55 and 4.67 times respectively at pH 4.7 and 1.68, 1.85 and 1.98 times respectively at pH 7.4. Increase in the emission intensity after the addition of DNA indicated that all compounds interacted with DNA through intercalative mode of interaction [30, 31]. In the case of hydrophobic intercalation, compound being packed into the base stack of the DNA–helix, will favor deactivation or de-excitation via fluorescence emission instead of radiation less deactivation which is prominent in the free rotating molecules [26]. Hence a significant increase in the fluorescence emission intensity of compound will be observed. This phenomenon directly infers that the interaction of drug to DNA has resultantly increased the quantum efficiency of interacting compound [26]. The enhancement in the fluorescence intensities may further be attributed to the fact that all the compounds are protected from the water molecules by the hydrophobic microenvironment of nitrogenous bases inside the DNA-helix on one hand and their mobility is restricted at the binding sites on the other hand. Resultantly, this masking of the compound fluorophore along with snaring at binding sites, upon interaction between the stacked bases within the helix or

surface binding at the reactive nucleophilic sites on the heterocyclic nitrogenous base of DNA molecule reduce the vibrational mode of relaxation after excitation and then the compound binding to DNA leads to marked increase in fluorescence emission intensity [32].

Fig. 2

3.3. DNA binding study by cyclic voltammetry

Cyclic voltammetry is one of the important and most popular electrochemical techniques for DNA binding studies with a fact that compound bound to DNA is redox active [4, 33]. Electrochemical behavior of three compounds APA-1, APA-2 and APA-3 were investigated using cyclic voltammetric technique in ethanol-water mixture (7:3) at scan rate of 100 mV/s and at glassy carbon electrode surface. All compounds showed irreversible reduction processes and a single peak was observed at reduction potential (E_{Pc}) of −0.897V, −0.926V, −0.874V, respectively at pH 4.7 and −0.963V, −0.977V, −0.95V, respectively at pH 7.4. Peak broadening was observed for all the compounds at both pH, which may be attributed to one step two electrons reduction process [33].

Cyclic Voltammograms were recorded after the addition of 10 μM to 60 μM DNA on optimized concentration (2.8×10^{-5} M) of APA-1, APA-2 and APA-3 at both pH values. Voltammetric responses have shown a decrease in peak height along with a shift of reduction peak towards more negative potential, Fig. 3. This behavior is suggestive of interaction of investigated compounds with DNA via intercalation [4, 33]. The voltammetic parameters obtained for the three compounds without and in the presence of DNA are given in Table 1.

Fig. 3 and Table 1

Randles-Sevick equation is used to determine the diffusion coefficient values of APA-1, APA-2 and APA-3 without and in the presence of DNA [34, 35].

$$I_p = 2.99 \times 10^5 \, n(\alpha n_\alpha)^{1/2} A C_o^* D_o^{1/2} \nu^{1/2} \quad (1)$$

where, I_p is peak current in amperes (A), n is charge transfer number, n_α is number of electrons transferred up to and including the rate determining step, α is transfer coefficient, A is surface area of the electrode (cm^2), C_o^* is bulk concentration of the electro active species (mol cm^{-3}), υ is potential scan rate in Vs^{-1} and D_o is diffusion coefficient ($cm^2 s^{-1}$).

I_p values were plotted *vs.* $\upsilon^{1/2}$ for all compounds without and in the presence of DNA which showed linear dependency of peak currents on the square root of scan rates, Fig. 4 (only shown for all the compounds at pH 4.7, and at pH 7.4 provided as Fig. S5 in supplementary information). The linearity of plots verified that main mass transport of these electro active species and their DNA bound complexes is diffusion controlled [36]. A negative shift in the peak potential along with increase in peak current by increasing the scan rate may further be attributed to irreversible nature of redox process [37] occurring in compounds with and without the addition of DNA, Figs. S6a & S6b (in supplementary information). Transfer coefficient (α) was calculated using equation; $E_p - E_{p/2} = 47.7 \text{ mV}/\alpha n$. For all the compounds its value was found lesser than 0.5 which suggests that redox reaction of compounds is irreversible process and two electrons are involved in the one step reduction process [38].

The diffusion coefficients of compounds APA-1, APA-2 and APA-3 before and after the addition of DNA were calculated and given in Table 2. The lower diffusion coefficients (D_o) values of DNA bound organotin carboxylates are responsible for the decay of peak current in cyclic voltammograms, Fig. 4.

Fig. 4 and Table 2

3.4. Evaluation of binding constants of compounds to DNA by UV-spectroscopy

Binding constant "K_b" of compound–DNA complex can be determined from the variation in absorbance in UV-visible spectra before and after the addition of DNA. Binding constants for the three compounds were evaluated spectrophotometrically under physiological conditions of pH (4.7 and 7.4) and temperature (37 °C) by applying Benesi-Hildebrand equation [4, 5, 39].

$$\frac{A_o}{A-A_o}=\frac{\varepsilon_G}{\varepsilon_{H-G}-\varepsilon_G}+\frac{\varepsilon_G}{\varepsilon_{H-G}-\varepsilon_G}\frac{1}{K_b\left[DNA\right]} \quad (2)$$

Where A_o and A are the absorbance's of compound and complex respectively, E_G and $E_{H\text{-}G}$ the molar extinction coefficients of compound and complex respectively. From the plot of $A_o/(A\text{-}A_o)$ to 1/[DNA], the ratio of the intercept to the slope gave the values of binding constant, K_b, Fig. 5.

The Binding constant values were calculated and given in Table 3. The order of magnitude of binding constant K_b at both the pH values (10^4 M^{-1}) for all the investigated compounds with DNA revealed their stronger binding via intercalation and is in agreement with that reported for typical intercalator lumazine (K = 1.74 × 10^4 M^{-1}) and anthracycline molecules ($K \approx 10^4 - 10^5$ M^{-1}) [39, 40]. Binding constants at stomach pH (4.7) for all the compounds were evaluated greater, while at pH 7.4 compound APA-3 showed comparatively greater binding constants than that of typical intercalator lumazine, Table 3. Further, the spectral changes in absorption spectra during compound–DNA complex formation in present work inferred intercalation as possible mode of interaction. In addition, the greater binding constants of investigated compounds at both the pH values may be attributed to their structural planarity due to phenyl groups in the investigated compounds.

Binding constants values are used to assess of stability of compound–DNA complexes. In present studies all the compounds showed greater values of binding constants and revealed the formation of their stable complexes with the DNA at both the pH. Among the two pH (stomach; 4.7 and blood; 7.4), however, all compounds bound to DNA more strongly at stomach pH as evident from comparatively greater K_b values at this pH (4.7), Table 3. Conversely, APA-3 showed relatively greater K_b value at both pH than that of APA-1 and APA-2. The strong affinity of APA-3 for DNA as indicated by its greater binding constant value as compared to APA-2 could be attributed to additional hydrophobic interactions of the bulky butyl moiety with the nucleotide bases of DNA [33]. Furthermore, the greater K_b value of APA-2 as compared to APA-1 is ascribed to the presence of extended aromatic system which may bind strongly with DNA [33]. The order of binding constants at pH 4.7 and pH 7.4 are given below.

$K_{\text{APA-3}} > K_{\text{APA-2}} > K_{\text{APA-1}}$ (At both stomach 4.7 and blood 7.4 pH)

and

$K_{\text{APA-3}}$ (stomach; 4.7 pH) > $K_{\text{APA-3}}$ (blood; 7.4 pH)

Using the data of binding constant, K_b, Gibbs free energy changes (ΔG) of compounds–DNA complexes were calculated from Eq. 3. Gibbs free energy change indicates the spontaneity/non- spontaneity of compound–DNA binding.

$$\Delta G = -RT\ln K_b \ (\text{kJ mol}^{-1}) \quad (3)$$

Free energies of all the compounds at both pH were evaluated as negative values showing the spontaneity of compounds–DNA interaction, Table 3 [4, 5, 41]. However, results indicated that APA-3 bind to the DNA more spontaneously as compared to other compounds at both pH values. The order of ΔG values of the compounds–DNA complexes at both pH is evaluated same as for binding constant values i.e.

$\Delta G_{APA-3} > \Delta G_{APA-2} > \Delta G_{APA-1}$ (At both stomach 4.7 and blood 7.4 pH)

and

ΔG_{APA-3} (stomach; 4.7 pH) > ΔG_{APA-3} (blood; 7.4 pH)

Fig. 5 and Table 3

3.5. Evaluation of binding constants and binding sites of compounds to DNA by fluorescence-spectroscopy

Since fluorescence emission intensity is varied after addition of DNA, the binding constant "K_b" of pro-drug–DNA complex can be determined from the variation in fluorescence emission intensity spectra. Binding constant "K_b" and binding stoichiometry have been evaluated spectrophotometrically by using following equation (8) [30].

$$\log \frac{F - F_o}{F} = \log K_b + n \log [DNA] \quad (4)$$

where, F_o and F are the fluorescence intensities of the fluorophore in the absence and in the presence of different concentrations of DNA, respectively. K_b and n are the binding constant and binding site size (binding stoichiometry) respectively which were determined by plotting log [(F-F_o)/F] *vs.* log [DNA], Fig. 6 (only shown for APA-3–DNA at both pH and at 37 °C, others provided as Fig. S7 in supplementary information).

Binding constant, binding site size values of all the compounds were calculated and given in Table 4. The data obtained for K_b from fluorescence spectroscopy was in good agreement with that obtained from UV-results and further verified the formation of most stable APA-3–DNA complex at stomach pH and good binding of all the investigated compounds with DNA at both pH values. The binding site size (n) was evaluated slightly greater than 1 (n>1) for all the compound–DNA complexes, Table 4, hence along with intercalation mode of binding the

possibility of groove binding and electrostatic binding could not be ignored [4, 28]. This suggest that ligand acid and its organotin complexes might have binding with DNA double helix through hydrogen bonding and planar phenyl groups present in investigated compounds [42].

From the binding constant data, the standard Gibbs free energy changes for all the compounds were calculated, Table 4. The negative values of ΔG through fluorescence results further lend supported the UV- results of free energy changes and indicated the spontaneity of all the compounds–DNA binding. The orders of K_b and ΔG values of the compounds–DNA complexes at both pH were found similar as obtained by UV- spectroscopy.

Fig. 6 and Table 4

3.6. Evaluation of binding constants and binding sites of compounds to DNA by cyclic voltammetry

Based upon the decrease in peak current of compounds by the addition of different concentration of DNA, the binding constants, K_b, for the three compound–DNA complexes were calculated according to the following equation [43].

$$I_p^2 = \frac{1}{K_b[DNA]}(I_{po}^2 - I_p^2) + I_{po}^2 - [DNA] \quad (5)$$

Where K_b is the binding constant, I_p and I_{po} are the peak currents with and without DNA. A plot of I_p^2 *vs.* ($I_{po}^2 - I_p^2$)/ [DNA] gave a straight line with a slope equal to the reciprocal of binding constant, K_b, Fig. 7 (only shown for APA-3–DNA at both pH and at 37 °C others provided as Fig. S8 in supplementary information).

The Binding constants of all the compounds were calculated. Comparatively stronger binding of all the compounds with DNA at stomach pH, and among all the compounds the greater K_b value for APA-3–DNA binding at stomach pH is evident from the data presented in Table 5. K_b values

obtained through voltammetic parameters were also found in good agreement with that obtained from UV- and fluorescence results hence confirming the compatibility of *binding constant* results from all the three complementary techniques. Gibbs free energy changes evaluated through K_b data using CV parameters were found as negative values as obtained through UV- and fluorescence results and further inveterate the involvement of spontaneous process in compound–DNA binding, Table 5. The order in the values of binding constant as well as free energy change was found identical as obtained by both spectroscopic techniques at both pH.

Binding site sizes (n) were evaluated through cyclic voltammetry by using following equation [44].

$$C_b / C_f = K\,[\text{free base pairs}] / s \quad (6)$$

Where, s is the binding site size in terms of base pairs (bp). Measuring the concentration of DNA in terms of compound concentration, the concentration of the base pairs can be expressed as [DNA] / 2. So Eq. (5) can be written as:

$$C_b / C_f = K\,[\text{DNA}] / 2s \quad (7)$$

C_f and C_b denote the concentration of the free and DNA bound species respectively. The C_b / C_f ratio was determined by the equation given below [45].

$$C_b / C_f = I - I_{DNA} / I_{DNA} \quad (8)$$

where I and I_{DNA} represent the peak currents of the compound in the absence and in the presence of DNA, respectively. Putting the value of K_b as calculated according to Eq. (5), the binding site size was obtained from the plot of $I - I_{DNA} / I_{DNA}$ *vs.* [DNA], Fig. 8 (only shown for APA-3–DNA at both pH and at 37 °C, others provided as Fig. S9 in supplementary information).

The binding site size (n) was evaluated slightly greater than 1 (n>1) for all the compound–DNA complexes, Table 5, the reason being same as discussed in previous section. The values of n obtained at both pH are consistent with that obtained through fluorescence spectroscopy.

Fig. 7, 8 and Table 5

3.7. Verification of DNA-binding studies of compounds by viscosity measurements

The viscosity measurement is one of the most reliable methods to verify different modes of DNA binding [46]. Generally for intercalation mode the viscosity of DNA solution increases upon addition of various concentrations of the compound. This increase in relative viscosity is due to the lengthening of DNA helix as the size of base pair pockets is increased to accommodate the compound as observed for a classical intercalator, ethidium bromide. In the present study, an increase in the relative viscosity of DNA at both stomach (4.7) and blood (7.4) pH was observed when various concentrations of the investigated compound (APA-1, APA-2 and APA-3) were added. This behavior is attributed to intercalative binding mode of the compounds with DNA and could be ascribed as enhancement in the length of DNA helix [47, 48]. The values of the relative specific viscosities for the compounds i.e. $(\eta / \eta_o)^{1/3}$ were plotted against [compound] / [DNA], Fig. 9, where η_o and η are the specific viscosity contributions of DNA in the absence and in the presence of the investigated compounds respectively. Increasing tendency in the viscosity curve upon addition of various concentrations of compound to DNA provided stronger evidence for the intercalation and further verified intercalative mode of binding as investigated though spectroscopic and electrochemical studies in the present work.

Fig. 9

3.8. Biological studies of compounds

3.8.1. DPPH free radical scavenging assay

To estimate the antioxidant potential of test compounds, DPPH free radical scavenging assay was used. The degree of discoloration of DPPH indicates the scavenging potential of the antioxidant compound. DPPH assay measures loss of DPPH color after reacting with the test compounds spectrophotometrically at 517 nm. The absorbance of DPPH at 517 nm decreases as color changes from purple to yellow due to scavenging of the free radical by the antioxidant. In this assay none of the synthesized compounds showed significant DPPH free radical scavenging activity at the concentrations tested. All the compounds have IC_{50} value >200 µg ml^{-1}.

3.8.2. Potato disc antitumor assay

The inhibition of *A. tumefaciens*-induced tumors (or Crown Gall) in potato disc tissue is an assay based on antimitotic activity, and can detect a broad range of known and novel antitumor effects [49]. This assay is based on the hypothesis that antitumor agents might inhibit the initiation and growth of tumors in both plant and animal systems, because certain tumorogenic mechanisms are similar in plants and animals [50]. The results obtained from potato disc antitumor assay and from other most commonly used antitumor screening assays had shown good correlation as tumor induction mechanisms are reported to be similar in both plants and animals [51]. All the compounds (APA-1, APA-2, and APA-3) were investigated against *Agrobacterium tumefaciens* (At 10) for their antitumor potentials. Assay was carried out at different concentrations (7.4, 22.2, 66.6 and 200 µg ml^{-1}) of synthesized compounds to examine whether an increase in concentration of compound influenced the tumor formation ability of bacterium and to calculate IC_{50} values. Vincristine (positive control) showed 100% tumor inhibition at all the concentrations tested whereas DMSO (negative control) has no interference with the activity of bacterium to induce tumors. Furthermore, the inhibition was observed in dose

dependent manner with highest inhibition at 200 μg ml^{-1} concentration. Antitumor activity can also be determined by 50% inhibitory concentration (calculated by inhibition curves of four concentrations tested for each compound). Lower the IC_{50} value more effective is the tested compound. An IC_{50} calculation favors APA-3 to be more active as compared to other compounds and exhibited best tumor inhibitory activity with lowest IC_{50} value of 7.37 μg ml^{-1}, Table 6. The effectiveness order of compounds is given as: APA-3 > APA-2 > APA-1.

Table 6

4. Conclusions

A carboxylic acid ligand (*Z*)-4-(4-acetylphenylamino)-4-oxobut-2-enoic acid (APA-1) and its compounds; triphenylstannyl (*Z*)-4-(4-acetylphenylamino)-4-oxobut-2-enoate (APA-2), and tri- n-butylstannyl (*Z*)-4-(4-acetylphenylamino)-4-oxobut-2-enoate (APA-3) were synthesized and characterized. All compounds were further investigated for their binding with ds.DNA through complimentary techniques; UV-visible spectroscopy, fluorescence spectroscopy, cyclic voltammerty and further verified for binding mode by viscosity measurements. The results obtained from these techniques under physiological conditions of pH {stomach (4.7) and blood (7.4)} and temperature (37°C) revealed predominant intercalation of the compounds within DNA. The negative values of standard Gibbs energy changes (ΔG) indicated the spontaneity of the binding of compounds with DNA. Interactional parameter, K_b, calculated from both spectroscopic techniques and cyclic voltammerty were in good agreement and indicated stronger binding and formation of compound–DNA complexes. The values of binding site size (n) calculated from fluorescence and voltammertric data further demonstrated the dominancy of intercalative mode for all the compound–DNA complexes. K_b, n and ΔG

values for all the compounds–DNA complexes inferred comparatively greater binding and spontaneity of APA-3 complex with DNA at both pH. Compounds were also probed for their antioxidant and antitumor activities through biological assays. All the compounds were found inactive for their antioxidant activity, while APA-3 showed greater antitumor activity as compared to other compounds. Results obtained for antitumor potential and DNA binding studies (K_b values) are correlated with each other and further justify the significance of present studies. Authors are assured that such studies and further investigations in this direction would not only help to predict the mechanism of action of investigated compounds with DNA as intracellular target but may lead to explore new and effective candidates as anticancer drug.

Associated Content

Supporting information

Figures S1 to S9 as supplementary information for DNA binding studies.

Author information

Corresponding Author

*E-mail: nasimaa2006@yahoo.com

Acknowledgements

This work is supported by Department of Chemistry, Faculty of Science, Allama Iqbal Open University Islamabad, Pakistan.

References

[1] M.S. Cooke, M.D. Evans, M. Dizaroglu, Oxidative DNA damage: mechanisms, mutation, and disease, J. Lunec, FASEB 17(2003) 1195–1214.

[2] P.C.A. Bruijnincx, P.J. Sadler, New trends for metal complexes with anticancer activity,

Curr. Opin. Chem. Biol. 12 (2008) 197–206.

[3] G.Gasser, I. Ott, N.M. Nolte, Organometallic Anticancer Compounds, J. Med. Chem. 54 (2011) 3–25.

[4] N. Arshad, U. Yunus, S. Razzque, M. Khan, S. Saleem, B. Mirza, N. Rashid, Electrochemical and spectroscopic investigations of isoniazide and its analogs with ds.DNA at physiological pH: evaluation of biological activities, Eur. J. Med. Chem. 47 (2012) 452–461.

[5] N. Arshad, N. Abbas, M.H. Bhatti, N. Rashid, M.N. Tahir, S. Saleem, B. Mirza, Synthesis, crystal structure, DNA binding and *in vitro* biological studies of Ni(II), Cu(II) and Zn(II) complexes of N-phthaloyglycine, J. Photochem. Photobiol. B: Biol, 117 (2012) 228–239.

[6] A.H. Pathan, R.P. Bakale , G.N. Naik, C.S. Frampton, K.B. Gudasi, Synthesis, crystal structure, redox behavior and comprehensive studies on DNA binding and cleavage properties of transition metal complexes of a fluorosubstituted thiosemicarbazone derived from ethyl pyruvate, Polyhedron 34 (2012) 149–156.

[7] S. Tabassum, W.M.A. Asbahy, M. Afzal, F. Arjmand, Synthesis, characterization and interaction studies of copper based drug with Human Serum Albumin (HSA): Spectroscopic and molecular docking investigations, J. Photochem. Photobiol. B: Biol. 114 (2012) 132–139.

[8] Z. Rehman, A. Shah, N. Muhammad, S. Ali, R. Qureshi, A. Meetsma, I.S. Butler, Synthesis, spectroscopic characterization, X-ray structure and evaluation of binding parameters of new triorganotin(IV) dithiocarboxylates with DNA. Eur. J. Med. Chem. 44 (2009) 3986–3993.

[9] C.E. Carraher Jr., C.U. Pittman Jr., Macromolecules Containing Metal and Metal-Like Elements, Volume 3: Biomedical Applications, edited by Alaa S. Abd-El-Aziz, Charles E. Carraher Jr., Charles U. Pittman Jr., John E. Sheats, and Martel Zeldin ISBN: 0-471-66737-4 Copyright © 2004 John Wiley & Sons, Inc., Chapter 1, pp 2–16.

[10] N. Muhammad, A. Shah, Z. Rehman, S. Shuja, S. Ali, R. Qureshi, M. Auke, M.N. Tahir, Organotin(IV) 4-nitrophenylethanoates: Synthesis, structural characteristics and intercalative mode of interaction with DNA, J. Orgamomet. Chem, 649 (2009) 3431–3437.

[11] M. Gielen, Tin-based antitumour drugs, Coord. Chem. Rev.15 (1996) 41–51.

[12] S. Tabassum, C. Pettinari, Chemical and biotechnological developments in organotin cancer chemotherapy, J. Organomet. Chem. 691(2006) 1761–1766.

[13] L. Pellerito, L. Nagy, Organotin(IV)$^{n+}$ complexes formed with biologically active ligands: equilibrium and structural studies, and some biological aspects, Coord. Chem. Rev. 224 (2002) 111–150.

[14] M. Gielen, Organotin compounds and their therapeutic potential: a report from the Organometallic Chemistry Department of the Free University of Brussels, Appl. Organomet. Chem., 16, (2002) 481–494.

[15] C. Pettinari, F. Marchetti, "Chemical and Biotechnological Development in Organotin Cancer Chemotherapy", in Tin Chemistry: fundamental, Frontiers and Applications, (ed.,) M. Gielen, A. Davies, K. Pannell, E.R.T. Tiekink, John Wiely & Sons, 2008. pp. 454–468.

[16] D. Du, Z. Jiang , C. Liu, A.M. Sakho, D. Zhu, L. Xu, Macrocyclic organotin(IV) carboxylates based on benzenedicarboxylic acid derivatives: Syntheses, crystal structures and antitumor activities, J. Organomet. Chem. 696 (2011) 2549–2558.

[17] S.K. Hadjikakou, N. Hadjiliadis, Antiproliferative and anti-tumor activity of organotin compounds, Coord. Chem. Rev., 253 (2009) 235–249.

[18] M. Nath, M. Vats, P. Roy, "Synthesis, Spectral Characterization and Anticancer Screening of Triorganotin (IV) Carboxylates" in Chemistry for Sustainable Development, (ed.,) M. G. Bhowon, S. J.-Laulloo, H. L. K. Wah, P. Ramasami, Springer, 2012, Chapter 18.

[19] A. Alama, B. Tasso, F. Novelli, F. Sparatore, Organometallic compounds in oncology: implications of novel organotins as antitumor agents, Drug Discovery Today, 14 (2009) 500–508.

[20] T. S. B. Baul, S. Basu, D. de Vos, A.Linden, Amino acetate functionalized Schiff base organotin(IV) complexes as anticancer drugs: synthesis, structural characterization, and in vitro cytotoxicity studies, Invest. New Drugs 27 (2009) 419–431.

[21] J. Sambrook, E.F. Fritsch, T. Maniatis, Molecular Cloning: a laboratory manual. Cold Spring Harbor, New York, 1989.

[22] M.E. Reichmann, S.A. Rice, C.A. Thomas, P. Doty, A further examination of the molecular weight and size of deoxypentose nucleic acid, J. Am. Chem. Soc. 76 (1954) 3047–3053.

[23] S.S. Babkina, N.A. Ulakhovich, Complexing of heavy metals with DNA and new bioaffinity method of their determination based on amperometric DNA-based biosensor, Anal. Chem. 77 (2005) 5678–5685.

[24] H. Nawaz, Z. Akhter, S. Yameen, H.M. Siddiq, B. Mirza, A. Rifat, Synthesis and biological evaluations of some Schiff-base esters of ferrocenyl aniline and simple aniline J. Organomet. Chem. 694 (2009) 2198–2203.

[25] M.S. Ahmad, M. Hussain, M. Hanif, S. Ali, M. Qayyum, B. Mirza, Di- and triorganotin(IV) esters of 3,4-methylenedioxyphenylpropenoic acid: Synthesis, spectroscopic characterization and biological screening for antimicrobial, cytotoxic and antitumor activities, Chem. Bio. Drug. Des. 71 (2008) 568–576.

[26] V.G. Ruiz, A.I. Olives, M. Antonia, M.A. Martín, P. Ribelles, M.T. Ramos, J.C.Menéndez, Biomedical Engineering, Trends, Research and Technologies, Edited by Dr. Sylwia Olsztynska, ISBN 978-953-307-514-3, published in print edition January, 2011, pp. 65-90.

[27] X. Yang, G. L. Shen, R.Q. Yu, Studies on Intramolecular Charge Transfer Fluorescence Probe and DNA Binding Characteristics, Microchem. J. 62 (1999) 394– 404.

[28] Z. Xu, G. Bai, C. Dong, Studies on interaction of an intramolecular charge transfer fluorescence probe: 40-Dimethylamino-2,5-dihydroxychalcone with DNA, Bioorg. Med. Chem. 13 (2005) 5694–5699.

[29] K.W. Kohn, M. J. Waring, D. Glaubiger, C. A. Friedman, Intercalative Binding of Ellipticine to DNA, Cancer Res. 35 (1975) 71–76.

[30] N. Shahabadi, A. Fatahi, Multispectroscopic DNA-binding studies of a tris-chelate nickel(II) complex containing 4,7-diphenyl 10-phenanthroline ligands, J. Mol. Struct. 970 (2010) 90–95.

[31] F. Arjmand, A.Jamsheera, M. Afzal, S, Tabassum, Enantiomeric Specificity of Biologically Significant Cu(II) and Zn(II) Chromone Complexes Towards DNA, Chirality, 24 (2012) 977-986.

[32] X.Z. Feng, Z. Lin, L.J. Yang, C. Wang, C.L. Bai, Investigation of the interaction between acridine orange and bovine serum albumin, Talanta, 47 (1998) 1223–1229.

[33] S. Shujha , A. Shah, Z.-Rehman , N. Muhammad, S. Ali, R. Qureshi, N. Khalid, A. Meetsma, Diorganotin(IV) derivatives of ONO tridentate Schiff base: Synthesis, crystal structure, in vitro antimicrobial, anti-leishmanial and DNA binding studies, Eur. J. Med. Chem. 45 (2010) 2902–2911.

[34] J.E.B. Randles, A cathode ray polarograph, Trans. Faraday Soc. 44 (1948) 322–327.

[35] A. Sevcik, Oscillographic polarography with periodical trinagular voltage, Collec. Czech. Chem. Commun. 13 (1948) 349–377.

[36] S. Wang, T. Penz, C.F. Yang, Electrochemical determination of interaction parameters for DNA and mitoxantrone in an irreversible redox process, Biophys. Chem. 104 (2003) 239–248.

[37] E. Niranjana, R. Raghavendra Naik, B.E. Kumara Swamy, Yadav D. Bodke, B.S. Sherigara, H. Jayadevappa, B.V. Badami, Cyclic Voltammetric Investigations of 3-aryl-4-bromo Sydnone and its Derivatives at Glassy Carbon Electrode, Int. J. Electrochem. Sci., 3 (2008) 980–992.

[38] A. J. Bard, L.R. Faulkner, Electrochemical Methods: Fundamentals and Applications, 2nd Edition; John Wiley & Sons, Inc.: New York, 2001.

[39] M.S. Ibrahim, Voltammetric studies of the interaction of nogalamycin antitumor drug with DNA Anal. Chem. Acta 443 (2001) 63–72.

[40] M.S. Ibrahim, I.S. Shehata, A.A. Al-Nateli, Voltammetric studies of the interaction of lumazine with cyclodextrins and DNA, J. Pharm. Biomed. Anal. 28 (2002) 217–225.

[41] M. Aslanoglu, Electrochemical and Spectroscopic Studies of the Interaction of Proflavine with DNA, Anal. Sci. 22 (2006) 439–443.

[42] M. Sirajuddin, S. Ali, A. Haider, N.A. Shah, A. Shah, M. R. Khan, Synthesis, characterization, biological screenings and interaction with calf thymus DNA as well as electrochemical studies of adducts formed by azomethine [2-((3,5-dimethylphenylimino)-methyl)phenol] and organotin(IV) chlorides, Polyhedron, 40 (2012) 19–31.

[43] J. Niu, G. Cheng, S. Dong, Study on the kinetic process of the complex reaction between bilirubin and cyclodextrins, Electrochim. Acta 39 (1994) 2455–2460.

[44] M.T. Carter, M. Rodriguez, A.J. Bard, Voltammetric Studies of the Interaction of Metal-Chelates with DNA .2. Tris-Chelated Complexes of Cobalt(III) and Iron(II) with 1,10-Phenanthroline and 2,2'-Bipyridine, J. Am. Chem. Soc. 111 (1989) 8901–8911.

[45] M. Aslanoglu, C.J. Isaac, A. Houlton, B.R. Horrocks, Voltammetric measurements of the interaction of metal complexes with nucleic acids, Analyst 125 (2000) 1791–1798.

[46] N. Shahabadi, S. Kashanian, M. Mahdavi, N. Sourinejad, DNA Interaction and DNA Cleavage Studies of a New Platinum(II) Complex Containing Aliphatic and Aromatic Dinitrogen Ligands Bioinorg. Chem. Appl. Volume 2011 (2011), Article ID 525794, 10 pages.

[47] F. Liu, K. A. Meadows, D. R. McMillin, DNA-Binding Studies of Cu(Bcp)(2)+ and Cu(Dmp)(2)+ - DNA Elongation without Intercalation of Cu(Bcp)(2)+, J. Am. Chem. Soc. 115 (1993) 6699–6704.

[48] S. Shi, J. Liu, J. Li, K.-C. Zheng, X.-M. Huang, C.-P. Tan, L.-M. Chen, L.-N. Ji, Synthesis, characterization and DNA-binding of novel chiral complexes Δ- and Λ-$[Ru(bpy)_2L]^{2+}$ (L = *o*-mopip and *p*-mopip), J. Inorg. Biochem. 100 (2006) 385–395.

[49] J.L. McLaughlin, L. L. Rogers, The use of biological assays to evaluate botanicals, Drug Inf. J. 32 (1998) 513–524.

[50] P.S. Coker, J. Radecke, C. Guy, N.D. Camper, Potato tumor induction assay: A multiple mode of drug action assay, Phytomedicine 10 (2003) 133–138.

[51] A. Rehman, M.I. Choudhary, W.J. Thomsen, Bioassay Techniques for Drug Development, Harwood Academic Publishers: The Netherlands, 2001, p. 9.

Figure captions

Fig. 1. UV-Spectra for (A) APA-1, (B) APA-2, (C) APA-3 (2.8×10^{-5} M) without (a) and in the presence of 10 μM (b), 20 μM (c), 30 μM (d), 40 μM (e), 50 μM and (f) 60 μM DNA at pH 4.7 **(**left hand side) and pH 7.4 (right hand side) and at 37 °C. The arrow direction (a-f) indicates increasing concentrations of DNA.

Fig. 2. Fluorescence emission spectra for (A) APA-1, (B) APA-2, (C) APA-3 (2.8×10^{-5} M) without (a) and in the presence of 10 μM (b), 20 μM (c), 30 μM (d), 40 μM (e), 50 μM (f) 60 μM DNA at pH 4.7 (left hand side) and pH 7.4 (right hand side) and at 37 °C. The arrow direction (a-f) indicates increasing concentrations of DNA.

Fig. 3. Cyclic voltammogram for (A) APA-1, (B) APA-2, (C) APA-3 (2.8×10^{-5} M) without (a) and in the presence of 10 μM (b), 20 μM (c), 30 μM (d), 40 μM (e), 50 μM (f) 60 μM DNA at pH 4.7 (left hand side) and pH 7.4 (right hand side) and at 37 °C. The arrow direction (a-f) indicates increasing concentrations of DNA.

Fig. 4. Plots of I_p *vs.* $\upsilon^{1/2}$ for 2.8×10^{-5} M (a) APA-1, (b) APA-2 and (c) APA-3 at pH 4.7 (acetate buffer) in the absence (1) and in the presence of 60 μM DNA (2) at various scan rates (Vs^{-1}).

Fig. 5. Plots of A_o / $A\text{-}A_o$ *vs.* 1 / [DNA] for the application of Benesi-Hildebrand equation for calculation of compound–DNA binding constant at pH 4.7 and 7.4 and at 37 °C.

Fig. 6. Plots of log $[(F\text{-}F_o) / F]$ *vs.* log [DNA] for the calculation of APA-3–DNA binding constant and binding site size at pH 4.7 (a) and 7.4 (b) and at 37 °C.

Fig. 7. Plots of I_p^2 *vs.* $I_{po}^2 - I_p^2$ / [DNA] for calculation of binding constant of APA-3–DNA adducts at pH 4.7 (a) and 7.4 (b) and at 37 °C.

Fig. 8. Plots of I- I_{DNA} / I_{DNA} *vs.* [DNA] for determination of binding site size of APA-3–DNA adducts at pH 4.7 (a) and 7.4 (b) and at 37 °C.

Fig. 9. Plots of relative specific viscosity *vs.* [compound] / [DNA] for APA-1, APA-2 and APA-3 at pH 4.7 (a) and 7.4 (b) and at 37 °C.

Table 1

Voltammetric parameters of APA-1, APA-2 and APA-3 in the presence and absence of DNA at pH 4.7 and 7.4 and at body temperature (37 °C).

Complex code	pH 4.7					pH 7.4				
	ν/Vs^{-1}	[DNA] μM	I/μA	Shift in $E_{p/mV}$	Decrease in I (%)	ν/Vs^{-1}	[DNA] μM	I/μA	Shift in $E_{p/mV}$	Decrease in I (%)
APA-1	0.1	0	105.6	—	—	0.1	0	103.6	—	—
APA-1–DNA	0.1	60	75.4	20	40.1	0.1	60	76.5	16	35.4
APA-2	0.1	0	99.5	—	—	0.1	0	98.4	—	—
APA-2–DNA	0.1	60	63.4	44	56.9	0.1	60	65.7	38	47.7
APA-3	0.1	0	40.2	—	—	0.1	0	39.6	—	—
APA-3–DNA	0.1	60	23.6	51	70.3	0.1	60	24.5	47	61.6

% decrease in current = $\frac{(Ip - Ip_{\circ})}{Ip_{\circ}} \times 100$

Table 2

Diffusion coefficients of APA-1, APA-2 and APA-3, before and after the addition of DNA at pH 4.7 and 7.4 and at body temperature (37 °C).

Compound	D_o (cm^2s^{-1}) at pH 4.7		D_o (cm^2s^{-1}) at pH 4.7	
	before the addition of DNA	after the addition of DNA	before the addition of DNA	after the addition of DNA
APA-1	2.46×10^{-10}	1.25×10^{-11}	1.09×10^{-09}	6.82×10^{-12}
APA-2	2.70×10^{-10}	2.66×10^{-11}	6.53×10^{-10}	1.74×10^{-11}
APA-3	1.02×10^{-10}	5.85×10^{-11}	2.11×10^{-10}	$4.4\,1 \times 10^{-11}$

Table 3

Binding constants and free energy values for the compounds–DNA complexes from UV-spectrophotometric data at pH 4.7 and 7.4 and at body temperature (37 °C).

Complex Code	pH 4.7		pH 7.4	
	Binding constant K_b/M^{-1}	Free Energy (-ΔG) kJmol^{-1}	Binding constant K_b/M^{-1}	Free Energy (-ΔG) kJmol^{-1}
APA-1–DNA	2.03×10^4	25.56	1.05×10^4	23.86
APA-2–DNA	2.45×10^4	26.05	1.49×10^4	24.76
APA-3–DNA	5.63×10^4	28.19	2.29×10^4	25.87

Table 4

Binding constants and free energy values for the compounds–DNA complexes from fluorescence spectroscopic data at pH 4.7 and 7.4 and at body temperature (37 °C).

Complex Code	pH 4.7			pH 7.4		
	Binding constant K_b/M^{-1}	Binding site size (n)	Free Energy (-ΔG) kJmol^{-1}	Binding constant K_b/M^{-1}	Binding site size (n)	Free Energy (-ΔG) kJmol^{-1}
APA-1–DNA	1.70×10^4	1.06	25.106	1.45×10^4	1.05	24.695
APA-2–DNA	3.80×10^4	1.10	27.179	3.09×10^4	1.07	26.645
APA-3–DNA	$7.9\ 4\times 10^4$	1.16	29.078	6.49×10^4	1.15	28.546

Table 5

Binding constants and free energy values for the compounds–DNA complexes from voltammetric data at pH 4.7 and 7.4 and at body temperature (37 °C).

Complex Code	pH 4.7			pH 7.4		
	Binding constant K_b/M^{-1}	Binding site size (n)	Free Energy (-ΔG) kJmol^{-1}	Binding constant K_b/M^{-1}	Binding site size (n)	Free Energy (-ΔG) kJmol^{-1}
APA-1–DNA	1.94×10^4	1.09	25.4	1.61×10^4	1.03	24.9
APA-2–DNA	9.43×10^4	1.51	29.5	7.69×10^4	1.14	28.9
APA-3–DNA	9.91×10^4	2.41	29.6	7.94×10^4	1.47	29.1

Table 6:

Antitumor activity of the compounds as evaluated by potato disc antitumor assay and their IC_{50} values.

Sample code	IC_{50} (µg ml^{-1})
APA-1	85.64
APA-2	39.75
APA-3	7.37
Vincristine	0.003
DMSO	-

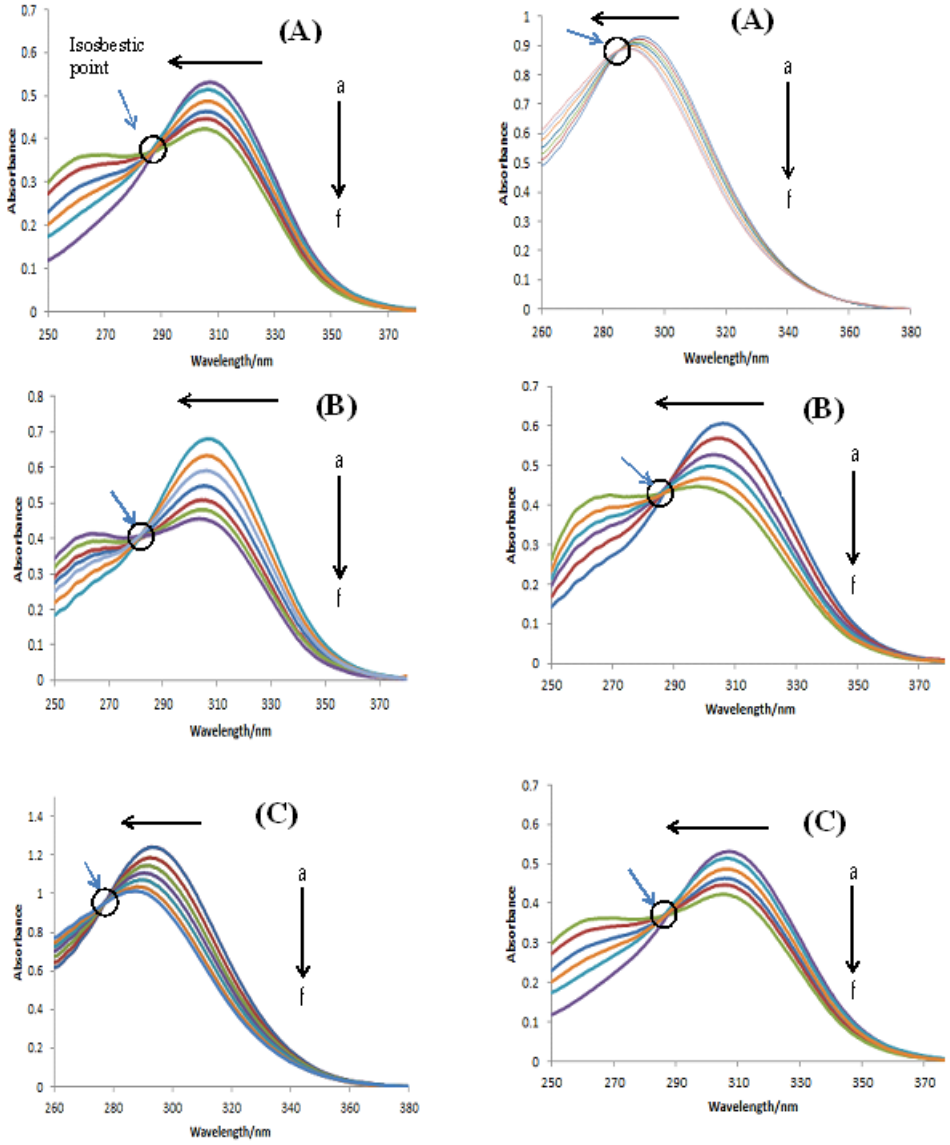

Fig. 1. UV-Spectra for (A) APA-1, (B) APA-2, (C) APA-3 (2.8×10^{-5} M) without (a) and in the presence of 10 μM (b), 20 μM (c), 30 μM (d), 40 μM (e), 50 μM and (f) 60 μM DNA at pH 4.7 **(**left hand side) and pH 7.4 (right hand side) and at 37 °C. The arrow direction (a-f) indicates increasing concentrations of DNA.

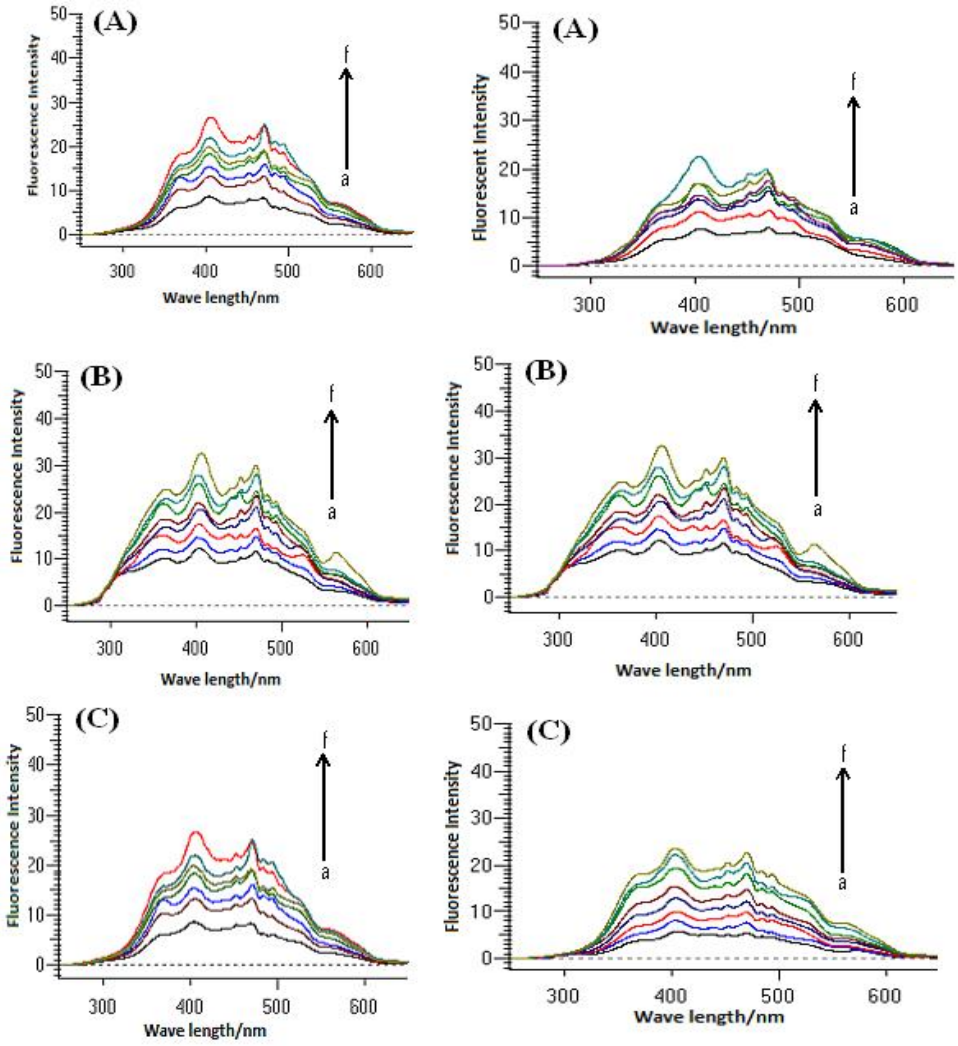

Fig. 2. Fluorescence emission spectra for (A) APA-1, (B) APA-2, (C) APA-3 (2.8×10^{-5} M) without (a) and in the presence of 10 μM (b), 20 μM (c), 30 μM (d), 40 μM (e), 50 μM (f) 60 μM DNA at pH 4.7 (left hand side) and pH 7.4 (right hand side) and at 37 °C. The arrow direction (a-f) indicates increasing concentrations of DNA.

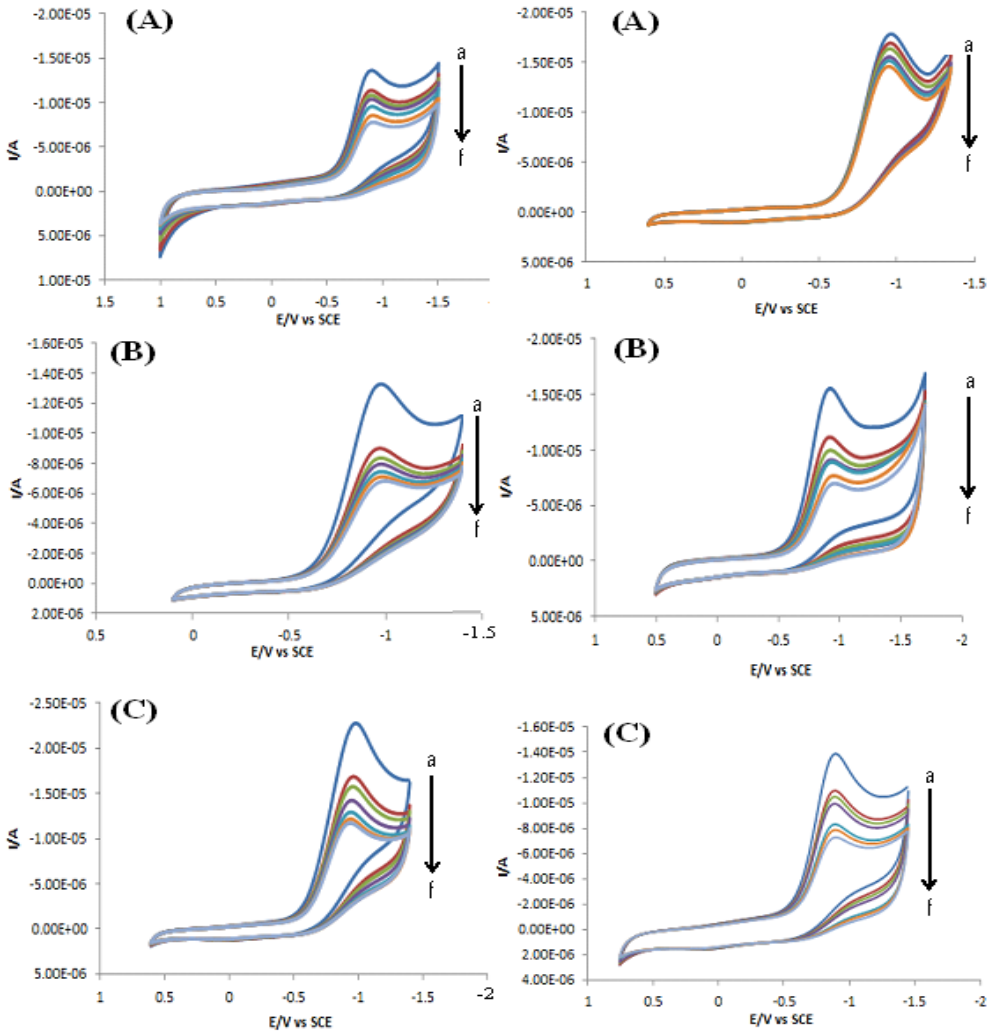

Fig. 3. Cyclic voltammogram for (A) APA-1, (B) APA-2, (C) APA-3 (2.8×10^{-5} M) without (a) and in the presence of 10 μM (b), 20 μM (c), 30 μM (d), 40 μM (e), 50 μM (f) 60 μM DNA at pH 4.7 (left hand side) and pH 7.4 (right hand side) and at 37 °C. The arrow direction (a-f) indicates increasing concentrations of DNA.

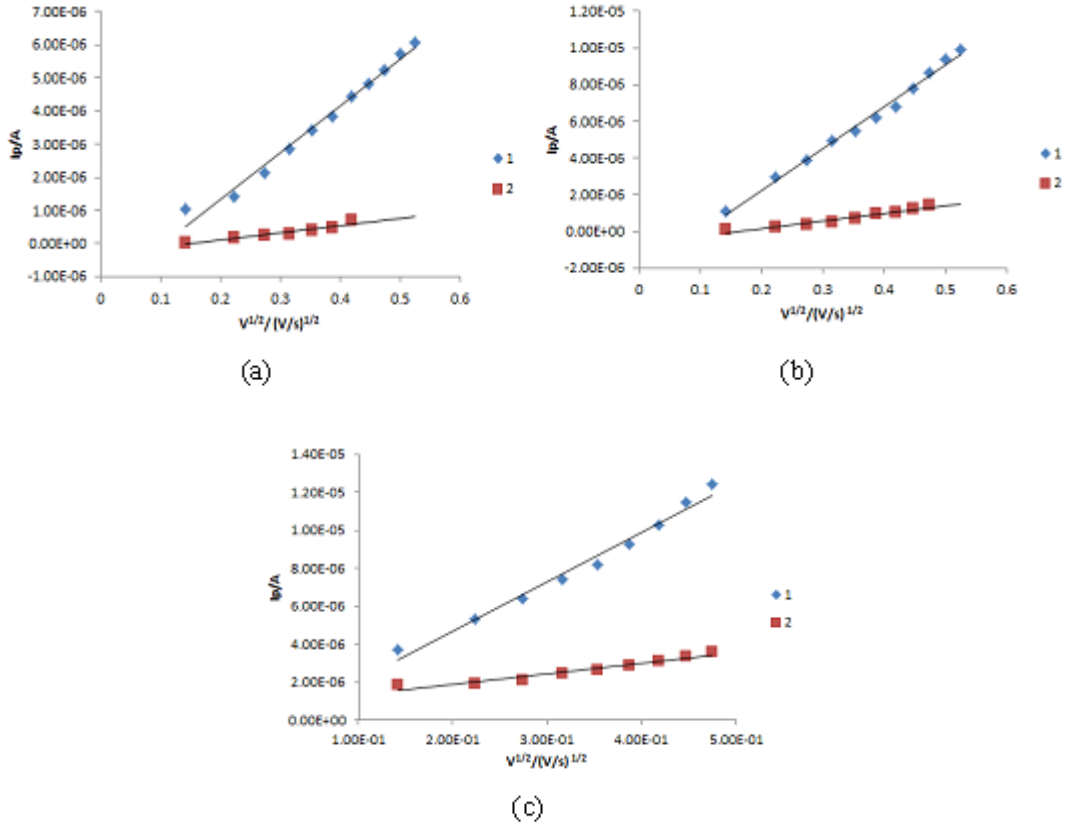

Fig. 4. Plots of I_p *vs.* $\upsilon^{1/2}$ for 2.8×10^{-5} M (a) APA-1, (b) APA-2 and (c) APA-3 at pH 4.7 (acetate buffer) in the absence (1) and in the presence of 60 µM DNA (2) at various scan rates (Vs^{-1}).

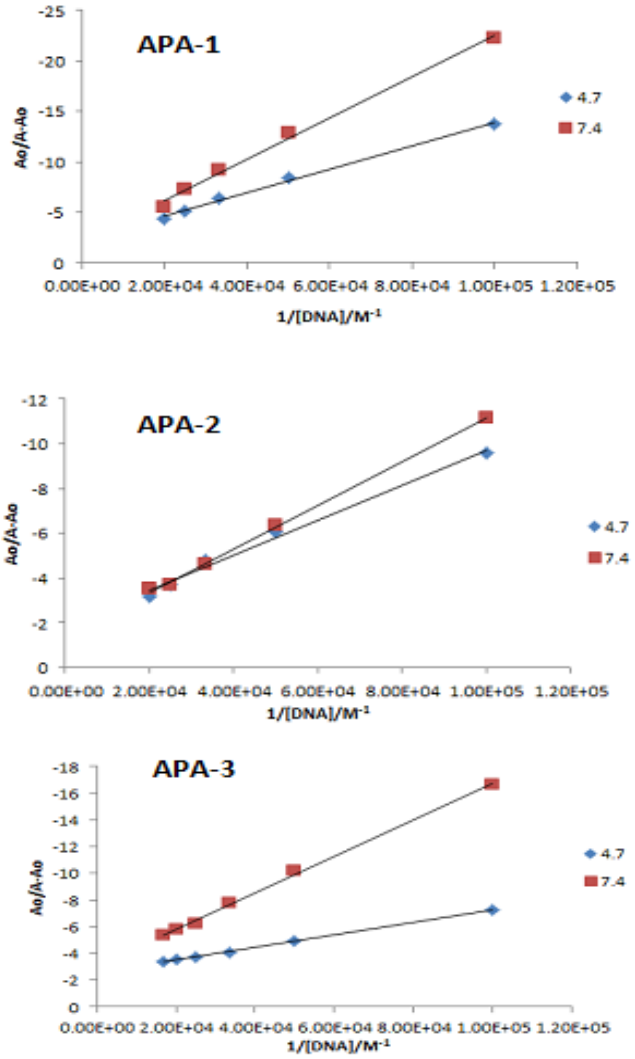

Fig. 5. Plots of A_o / A-A_o *vs*. 1 / [DNA] for the application of Benesi-Hildebrand equation for calculation of compound–DNA binding constant at pH 4.7 and 7.4 and at 37 °C.

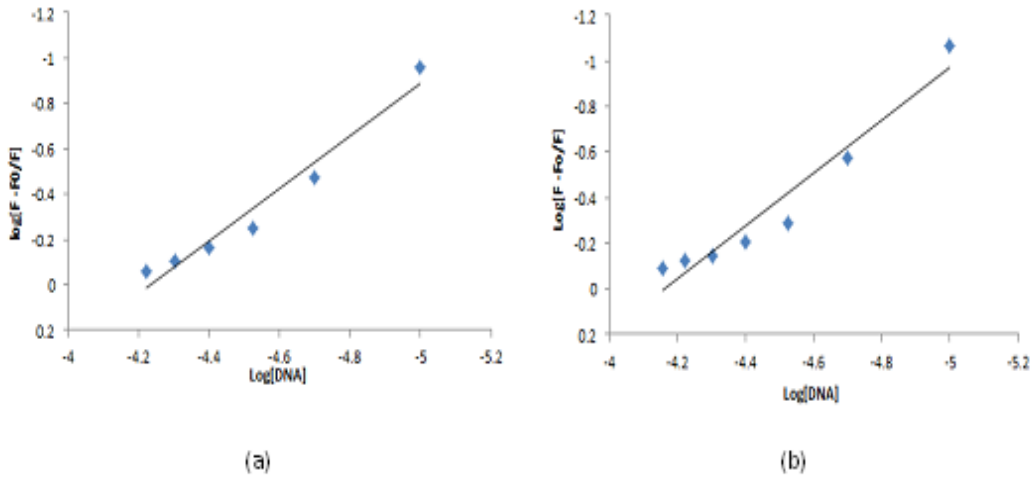

Fig. 6. Plots of log [(F-F_o) / F] *vs.* log [DNA] for the calculation of APA-3–DNA binding constant and binding site size at pH 4.7 (a) and 7.4 (b) and at 37 °C.

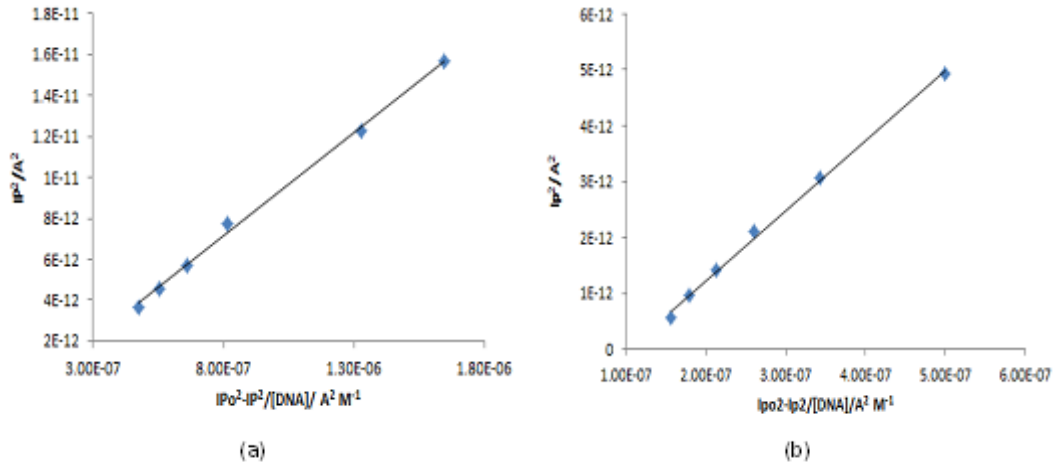

Fig. 7. Plots of I_p^2 *vs.* I_{po}^2- I_p^2/ [DNA] for calculation of binding constant of APA-3–DNA adducts at pH 4.7 (a) and 7.4 (b) and at 37 °C.

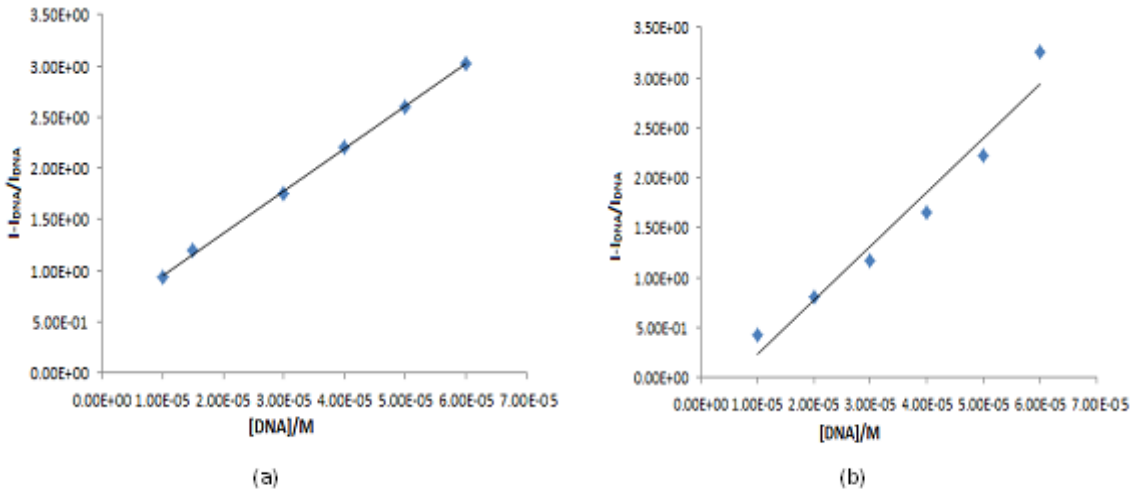

Fig. 8. Plots of I- I_{DNA} / I_{DNA} *vs.* [DNA] for determination of binding site size of APA-3–DNA adducts at pH 4.7 (a) and 7.4 (b) and at 37 °C.

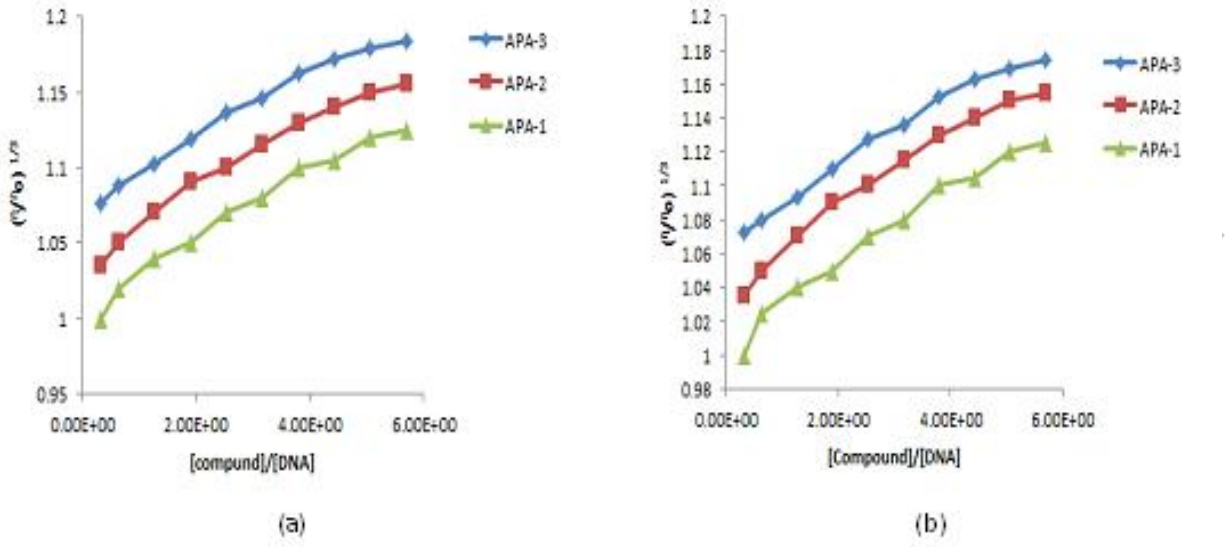

Fig. 9. Plots of relative specific viscosity *vs.* [compound] / [DNA] for APA-1, APA-2 and APA-3 at pH 4.7 (a) and 7.4 (b) and at 37 °C.

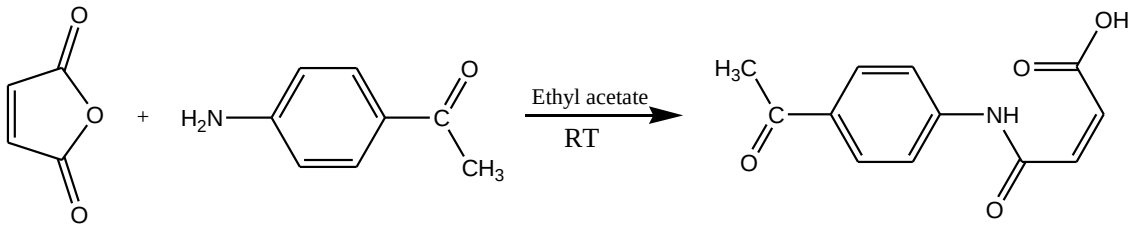

APA-1

Scheme 1

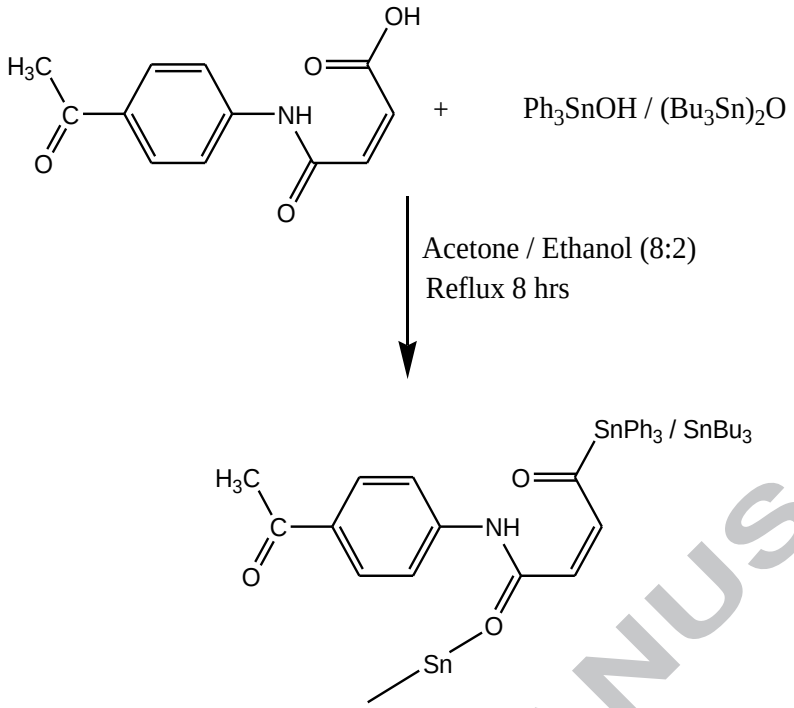

APA-2 (Ph_3Sn-), APA-3 (Bu_3Sn-)

Scheme 2

Graphical abstract (Pictogram)

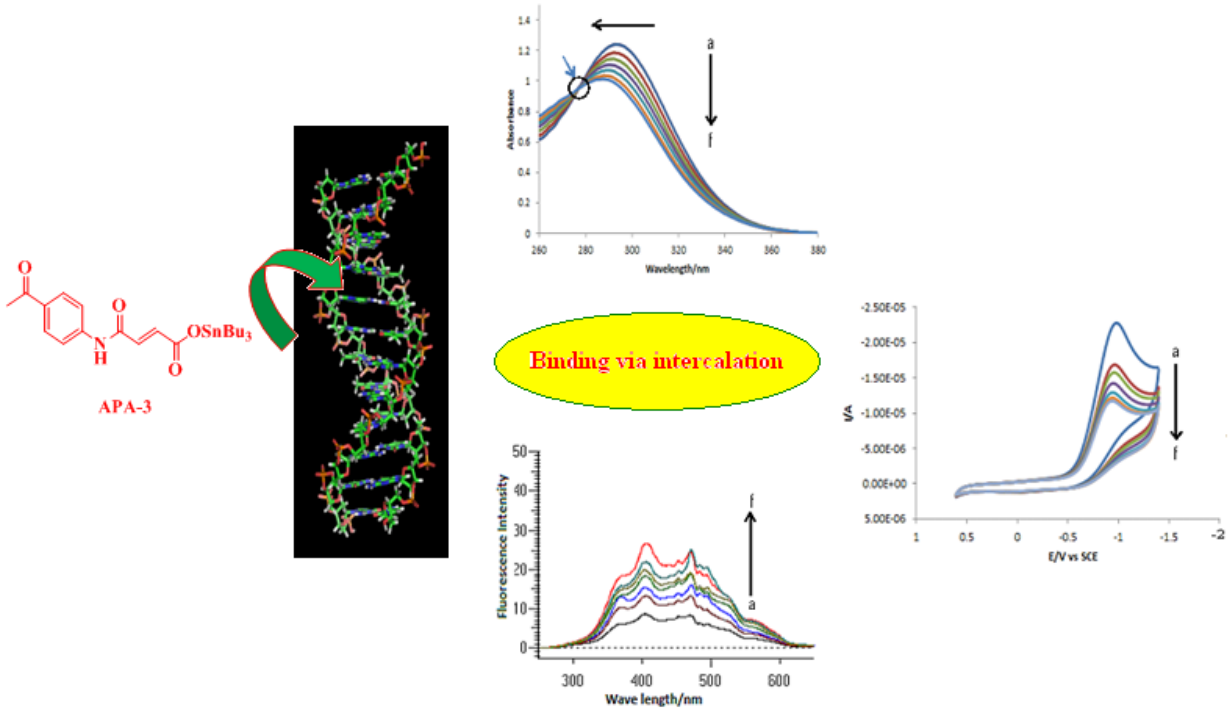

Graphical abstract (short note)

Carboxylic acid ligand and its triorganotin complexes; investigated for their binding with DNA and bioactivities. Among all tri-n-butyltin complex showed comparatively good DNA binding via intercalation and better antitumor potential.

Research highlights.

- Synthesis characterization of carboxylic acid ligand and its triorganotin complexes
- All compounds interact with DNA via intercalation
- Among all comparatively good DNA binding was investigated for APA-3 complex
- APA-3 complex showed better antitumor potential